Wnt Inhibitor Screen Reveals Iron Dependence of β-Catenin Signaling in Cancers

Siyuan Song[1], Tania Christova[1], Stephen Perusini[1], Solmaz Alizadeh[2], Ren-Yue Bao[1,8], Bryan W. Miller[1], Rose Hurren[3], Yulia Jitkova[3], Marcela Gronda[3], Methvin Isaac[4], Babu Joseph[4], Ratheesh Subramaniam[4], Ahmed Aman[4], Anh Chau[4], Donna E. Hogge[5], Scott J. Weir[6], James Kasper[7], Aaron D. Schimmer[3], Rima Al-awar[4], Jeff L. Wrana[2], and Liliana Attisano[1]

Abstract

Excessive signaling from the Wnt pathway is associated with numerous human cancers. Using a high throughput screen designed to detect inhibitors of Wnt/β-catenin signaling, we identified a series of acyl hydrazones that act downstream of the β-catenin destruction complex to inhibit both Wnt-induced and cancer-associated constitutive Wnt signaling via destabilization of β-catenin. We found that these acyl hydrazones bind iron *in vitro* and in intact cells and that chelating activity is required to abrogate Wnt signaling and block the growth of colorectal cancer cell lines with constitutive Wnt signaling. In addition, we found that multiple iron chelators, desferrioxamine, deferasirox, and ciclopirox olamine similarly blocked Wnt signaling and cell growth. Moreover, in patients with AML administered ciclopirox olamine, we observed decreased expression of the Wnt target gene AXIN2 in leukemic cells. The novel class of acyl hydrazones would thus be prime candidates for further development as chemotherapeutic agents. Taken together, our results reveal a critical requirement for iron in Wnt signaling and they show that iron chelation serves as an effective mechanism to inhibit Wnt signaling in humans. *Cancer Res; 71(24); 7628–39. ©2011 AACR.*

Introduction

Inappropriate activation of the canonical Wnt/β-catenin signaling pathway contributes to the development of a numerous human cancers (1–3). In colorectal cancers, loss-of-function mutations in the tumor suppressor, adenomatous polyposis coli (APC) are common. APC is an integral part of the destruction complex that controls cytoplasmic β-catenin levels by promoting ubiquitin-mediated degradation of β-catenin. Cancer-associated mutations in APC, thus lead to constitutively high levels of β-catenin and the concomitant expression of Wnt/β-catenin target genes that are important in cell growth, survival, and metastasis (1–3). In other cancers, constitutive Wnt signaling is achieved by a variety of means, such as increases in Wnt ligand or decreases in secreted inhibitors (2). Deregulation of the Wnt/β-catenin pathway has been reported in acute myeloid leukemias (AML) where expression of β-catenin is correlated with poor prognosis (4, 5). In addition, Wnt/β-catenin signaling has been shown to be required for the development of the highly proliferative leukemia stem cells (LSC), that are thought to maintain leukemias (6). The widespread deregulation of the Wnt pathway in diverse cancers makes it an attractive therapeutic target (7, 8) and while several chemical inhibitors of the Wnt pathway have been identified (7–11), there remains the need for effective small-molecule inhibitors appropriate for therapeutic development.

Cancer cells have an increased demand for iron to maintain robust cell proliferation, yet use of iron chelators for cancer treatment has only recently been rigorously considered (12–15). Here, we used a mammalian cell–based screen and identified a class of acyl hydrazones that block constitutive Wnt signaling and cell growth through their activity as iron chelators and thereby suggest that iron chelation–based therapies may be an effective means to target Wnt signaling in cancers.

Materials and Methods

Compounds

Compound 21H7 was purchased from Ryan Scientific, indirubin-3′-monoxime (I3M), desferioxamine, and dimethyloxallyl glycine (DMOG) from Sigma-Aldrich; deferasirox and ciclopirox olamine from ChemPacific Corporation; and M-110 (16), kindly provided by Jan Jongstra (Toronto Western Research

Authors' Affiliations: [1]Department of Biochemistry, Donnelly Centre for Cellular and Biomolecular Research, University of Toronto; [2]Centre for Systems Biology, Samuel Lunenfeld Research Institute; [3]Princess Margaret Hospital, Ontario Cancer Institute; [4]Medicinal Chemistry Platform, Ontario Institute for Cancer Research, Toronto, Ontario; [5]BC Cancer Research Centre, Vancouver, British Columbia, Canada; [6]Institute for Advancing Medical Innovation, The University of Kansas Cancer Center, Kansas City, Missouri; [7]The Leukemia and Lymphoma Society, White Plains, New York; and [8]College of Animal Sciences, Zhejiang University, Hangzhou, Zhejiang, China

Note: Supplementary data for this article are available at Cancer Research Online (http://cancerres.aacrjournals.org/).

Corresponding Author: Liliana Attisano, Department of Biochemistry, Donnelly CCBR, Room 1008, University of Toronto, 160 College Street, Toronto, Ontario, Canada M5S 3E1. Phone: 416-946-3129; Fax: 416-978-8548; E-mail: liliana.attisano@utoronto.ca

doi: 10.1158/0008-5472.CAN-11-2745

Institute, Toronto, ON, Canada), was synthesized by Sundia MediTech Company. OICR142 and OICR623 were synthesized by the OICR Medicinal Chemistry Group.

β-catenin-firefly luciferase stabilization assay and high throughput screen

HEK293 cells, stably expressing a Flag-β-catenin-firefly luciferase fusion protein were plated into 96-well dishes at 1,250 cell per well. The next day, cells were incubated 1 hour in Minimum Essential Media with 0.2% fetal calf serum, 1 hour with 1.2 μmol/L compounds, and then Wnt3A or control conditioned media, prepared as described (17, 18) was added for 16 hours. Luciferase activity was measured using Bright-Glo (Promega) 10 min after addition, using the CLIPR plate reader (Molecular Devices). Screens were conducted at the SMART Robotics Facility at the Samuel Lunenfeld Research Institute. Hits were identified by B-score analysis. For validation assays, Flag-β-catenin-firefly luciferase was immunoprecipitated from cell lysates with anti-Flag antibody and collected using Protein G beads.

Transcriptional reporter, electrophoretic mobility shift assay, and cell growth assays

Cell lines, from American Type Culture Collection, were expanded, frozen, and thawed aliquots cultured for less than 6 months. Cells were routinely tested for Mycoplasma, and Wnt pathway status was monitored using TOPFLASH/FOPFLASH. Cells were transfected with CMV-βgal and either 5×HRE-luciferase (provided by Dr. Michael Ohh, University of Toronto, Toronto, ON, Canada), TOPFLASH or FOPFLASH using calcium phosphate (HEK293T) or Lipofectamine 2000 (SW480, DLD-1, SW620, and HCT116). HEK293T cells were incubated with compounds for 1 hour prior to overnight incubation with control or Wnt3A-conditioned medium. For all other cells, compounds were added 5 hours posttransfection, and cells were incubated for 24 hours in full serum containing media. Luciferase activity, normalized to β-galactosidase activity was measured as previously (17, 18). All results were statistically significant ($P < 0.005$) using the Student 2-tailed t test at 5 and 10 μmol/L of compound. Iron responsive element (IRE)-binding activity of iron regulatory proteins (IRP) was analyzed by gel shift assay as described (19). Growth inhibition was determined at 72 hours using the Sulforhodamine B (SRB) assay as published (20).

GST-E-cadherin pull down assays and immunoblotting

For immunoblotting, cells were lysed and total protein content was measured by the Bradford assay (Bio-Rad). The following antibodies were used: anti-Flag M2, rabbit anti-Ferritin and anti-actin (Sigma-Aldrich), anti-β-catenin and anti-HIF1α (BD Biosciences), anti-active β-catenin (Millipore), and mouse anti-Transferrin Receptor (TfRI; Invitrogen). For glutathione *S*-transferase (GST) pull-downs, 3 μg of purified bacterially produced GST or GST-E-cadherin (cytoplasmic tail domain) protein (21), bound to glutathione beads, was incubated with whole cell lysates for 1 hour at 4°C to collect the free cytoplasmic pool of β-catenin. Beads were washed 3 times and analyzed by immunoblotting.

Measurement of intracellular calcein-chelatable iron

Cells were loaded with 100 μmol/L ferric ammonium citrate (FAC) for 24 hours (22), washed twice with PBS containing 20 mmol/L HEPES, pH 7.3, loaded with 0.25 μmol/L calcein green acetoxymethyl ester (calcein-AM; Molecular Probes) in serum-free medium containing 20 mmol/L HEPES, pH 7.3 for 15 minutes at 37°C, and then were washed and plated at 50,000 cells/well in a 96-well plate (23). Intracellular fluorescence intensity of calcein ($\lambda_{ex} = 485$ and $\lambda_{em} = 520$), a measure of the amount of labile iron (24), was determined as a function of time 1 minute before and 10 minutes after compound addition at 37°C using FLUOstar OPTIMA (BMG Labtech) microplate reader.

Microarray analysis and real-time PCR

SW480 cells were incubated with 10 μmol/L OICR623, 100 μmol/L desferioxamine or 50 μmol/L deferasirox or dimethyl sulfoxide (DMSO) as control for 6 hours. RNA was isolated using the PureLink Mini Kit (Invitrogen), and cDNA samples were hybridized to the GeneChip Human Gene 1.0 ST array (Affymetrix) and then scanned with the Affymetrix GeneChip Scanner 3000 at the Center for Applied Genomics. Raw data were prenormalized using RMA (robust multiarray average) algorithm, adjusted for batch effects and differentially expressed genes were identified using LIMMA (linear models for microarray data; ref. 25). Data are available at GEO (GSE32369). Real-time PCR was carried out using SYBR Green (Applied Biosystems) using validated primers (Supplementary Table S1). Gene expression was normalized to hypoxanthine phosphoribosyltransferase and relative quantitation was calculated using the $\Delta\Delta C_t$ method. Results shown are statistically significant ($P < 0.005$) using the Student 2-tailed t test.

Clinical trial of oral ciclopirox olamine in patients with refractory or relapsed hematologic malignancies

Patients were treated with ciclopirox olamine at increasing concentrations from 5 to 80 mg/m^2 daily for 5 days, in a phase I clinical trial, following informed consent and REB approval by the Princess Margaret Hospital, Toronto, Canada (NCT00990587). Peripheral blood samples were obtained before, during, and after drug treatment. Mononuclear cells were separated by Ficoll-Hypaque (Sigma Chemical) density-gradient centrifugation and AML blasts isolated by magnetic bead separation.

Results

Identification of small-molecule inhibitors of Wnt signaling

The deleterious effects of constitutive Wnt signaling result from abnormally high levels of β-catenin protein (1). Thus, to identify small-molecule inhibitors that reverse β-catenin accumulation, we designed a homogeneous high throughput screening (HTS) assay using HEK293 cells stably expressing a fusion protein comprising firefly luciferase (FFluc) linked to β-catenin in which fusion protein levels were measured using a luciferase assay (Fig. 1A). Cells were treated with compounds

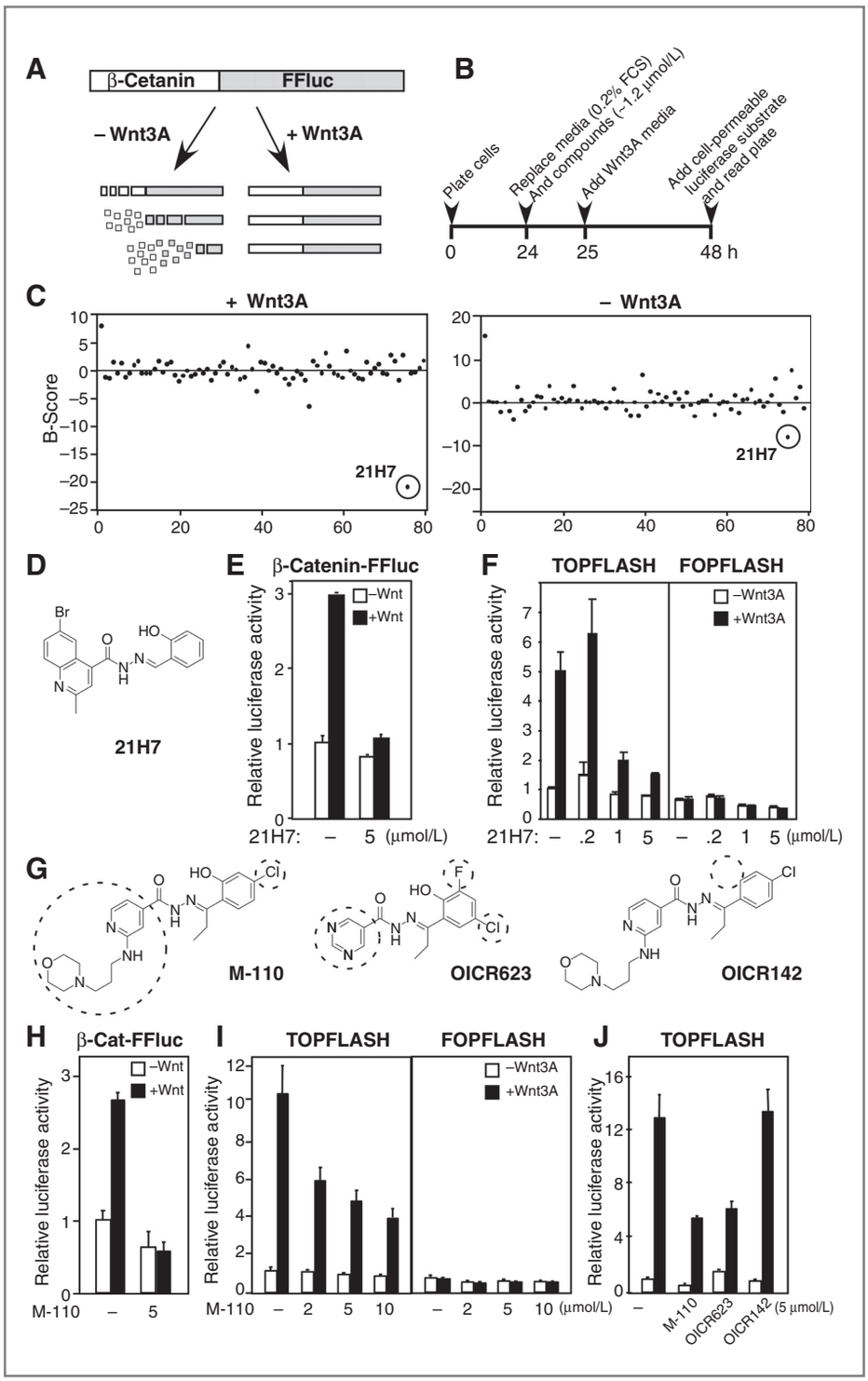

Figure 1. Identification of a Wnt/β-catenin inhibitor. A and B, Wnt/β-catenin pathway screen. The levels of a Flag-β-catenin-FFluc fusion protein stably expressed in HEK293 cells were measured by luciferase assay. C, results from duplicate 96-well plates in the presence and absence of added Wnt3A. B-score analyses identified compound 21H7. D and G, structures of the screen hit, 21H7 (D) and structural variants, M-110, OICR623, and OICR142 (G). E and H, inhibition of β-catenin stabilization. HEK293T cells stably expressing Flag-β-catenin-FFluc were treated overnight with 5 μmol/L 21H7 (E), 5 μmol/L M-110 (H), or DMSO (–) with or without Wnt3A. Following anti-Flag immunoprecipitation, β-catenin-FFluc levels were measured by luciferase assay. F, I, and J, inhibition of Wnt3A-dependent transcription. HEK293T cells were transfected with TOPFLASH or FOPFLASH and cultured overnight with or without Wnt3A and the indicated compounds. Promoter activity was measured by luciferase assay and is shown as the mean of 3 replicates ± SD. FCS, fetal calf serum.

for 1 hour and then cultured with or without Wnt3A for 16 hours before determining β-catenin-FFluc levels (Fig. 1B). Screening of 10,400 compounds from the Maybridge Collection (Fig. 1C) yielded 10 positive hits that were subsequently screened in a secondary assay for inhibition of the Wnt TOPFLASH reporter. One compound, 21H7, was identified as an inhibitor of the Wnt pathway that abrogated Wnt3A-dependent stabilization of β-catenin-FFluc and activation of TOPFLASH, but had no effect on FOPFLASH, a Wnt-insensitive mutant variant (Fig. 1D–F).

M-110, a structural variant of 21H7, also inhibited stabilization of β-catenin-FFluc and Wnt/β-catenin–dependent activation of TOPFLASH with no effect on FOPFLASH (Fig. 1G–I) as did compound OICR623, which contains the more polar pyrimidine group and a 2-fluoro-4-chloro phenolic moiety (Fig. 1G and J). In contrast, OICR142, which lacks the orthohydroxy group rendered the compound inactive (Fig. 1G and J). Thus, our screen identified a class of acyl hydrazones that inhibit Wnt-induced transcriptional responses.

Inhibition of Wnt/β-catenin signaling and cell proliferation in colorectal cancer cells

Most colorectal cancer cell lines display constitutive Wnt signaling because of mutations in APC. M-110 treatment of APC-mutant DLD-1 cells (26), preferentially attenuated constitutive TOPFLASH activity as compared with FOPFLASH, and had no effect on the CMV-β-galactosidase control reporter (Fig. 2A). Real-time PCR analysis also revealed that M-110 inhibited expression of the endogenous Wnt targets, AXIN2 and SP5 (Fig. 2B). In other APC mutant colorectal cancer cell lines, including SW480, SW620, and Colo205, M-110 similarly reduced TOPFLASH activity (Supplementary Fig. S1A) and expression of Wnt target genes (Fig. 2C). OICR623 and 21H7 also inhibited Wnt activity, whereas compound OICR142, which lacks the orthohydroxy group did not (Fig. 2D; see also Fig. 5). The Wnt/β-catenin pathway regulates cell proliferation in colorectal cancer cells. Consistent with this, M-110, OICR623, and 21H7 inhibited the growth of DLD-1 and SW480 cells, with IC_{50} values in the range of 0.5 to 1.7 μmol/L (Fig. 2E and Supplementary Fig. S1B). Thus, this family of small molecules inhibits constitutive Wnt signaling and blocks the growth of colorectal cancer cell lines.

Acyl hydrazones block Wnt signaling by promoting β-catenin degradation downstream of the destruction complex

There are 2 cellular pools of β-catenin, plasma membrane E-cadherin-associated and Wnt-modulated cytoplasmic pools (27). In mouse L cells, where most of the β-catenin is cytoplasmic, M-110, OICR623, and 21H7 blocked Wnt-induced stabilization of total β-catenin and the active, nonphosphorylated (S37/T41) β-catenin, which mediates Wnt signaling (Fig. 3A). In SW480 cells, M-110 also decreased the levels of free cytoplasmic β-catenin as determined by E-cadherin pull down assays, which collects β-catenin that is not prebound to E-cadherin, and reduced the pool of the active, nonphosphorylated β-catenin (Fig. 3B). Total β-catenin levels, which include the E-cadherin-bound pool were not significantly affected (Fig. 3B), nor were β-catenin mRNA levels (Supplementary Fig. S1C). Degradation of β-catenin occurs in a destruction complex comprising Axin and APC, within which CK1 and GSK3β-mediated phosphorylation of β-catenin marks it for ubiquitin-mediated degradation (1). DLD-1 and SW480 cells have a mutant APC, suggesting that the compounds act downstream of the destruction complex. Consistent with this, M-110 also blocked Wnt signaling when other destruction complex components were disrupted, including abrogation of AXIN1/2 expression using siRNAs or inhibition of GSK3β activity using LiCl or I3M (Fig. 3C and D). The ability of M-110 to decrease the levels of active β-catenin was mitigated in the presence of MG132, a proteasome inhibitor, but not by chloroquine, a lysosomal inhibitor (Fig. 3E), indicating ubiquitin-mediated degradation of β-catenin. M-110, OICR623, and 21H7 also inhibited activation of the TOPFLASH reporter in HCT116 cells, which harbor a constitutively-active version of β-catenin and in HEK293T cells overexpressing versions of β-catenin lacking the phosphorylation sites (Fig. 3F and G; Supplementary Fig. S1D). Altogether, these data show that the compounds act downstream of the destruction complex to destabilize active β-catenin.

Gene expression profiling reveals compounds induce an iron chelation signature

To gain insights into molecular mechanisms, we used microarrays to examine changes in gene expression in SW480 cells treated for 6 hours with OICR623. Analysis of results from replicate runs revealed that OICR623 significantly ($P < 0.05$) upregulated the expression of 31 genes by 1.5-fold or greater (Fig. 4A and B) including several genes induced by iron chelators (28), such as *DDIT4*, *VEGFA*, and *NDRG1*. This gene profile was next compared with that obtained using 2 well-described iron chelators, desferioxamine and deferasirox in cells treated in parallel. At 6 hours of treatment, 64 and 72 genes were upregulated by greater than 1.5-fold ($P < 0.05$) by desferioxamine and deferasirox, respectively, of which 64 overlapped (Fig. 4A). Remarkably, all 31 genes upregulated by OICR623 were found within the desferioxamine/deferasirox signature. Similar results were observed in the case of significantly (1.5-fold, $P < 0.05$) downregulated genes, although this overlap set comprised only 4 genes (Fig. 4B). Of note, at this early time point, inhibition of Wnt target gene expression was not yet manifested. These results thus show that the OICR623-induced gene signature is entirely encompassed by that of the iron chelators, desferioxamine and deferasirox.

Iron depletion inhibits the activity of iron-dependent enzymes, including prolyl hydroxylases (PHD), which promote stabilization of the hypoxia inducible transcription factor, HIF1α (29, 30). Treatment of SW480 and DLD-1 cells with OICR623, M-110, and 21H7, stabilized HIF1α and activated a HIF1α transcriptional reporter, 5xHRE-luciferase (Fig. 4C and D). Furthermore, genes induced by OICR623, desferioxamine, and deferasirox in the microarray analysis included the known HIF1α targets (29), *VEGFA*, *ADM*, *EGLN3*, and *NDRG1* (Fig. 4A). Verification of microarray results by real-time PCR showed that all 3 acyl hydrazones, OICR623, M-110, and 21H7, as well as the iron chelators, desferioxamine and deferasirox, rapidly induced expression of the iron-dependent and/or HIF1α target genes, *NDRG1*, *DDIT4*, *VEGFA*, and *GLUT1* in SW480 cells, used for the microarray study and in DLD-1 and SW620 cells (Fig. 4E and Supplementary Fig. S2A and S2B).

Under conditions of iron depletion, IRPs recognize and bind to IREs in mRNAs such as Ferritin (Ft), to stall translation or to TfRI mRNA to enhance mRNA stability and translation (14). As expected for iron chelators, treatment of SW480 cells with M-110 or deferasirox resulted in enhanced IRE–IRP binding activity, in an RNA-binding gel shift assay (Fig. 4F).

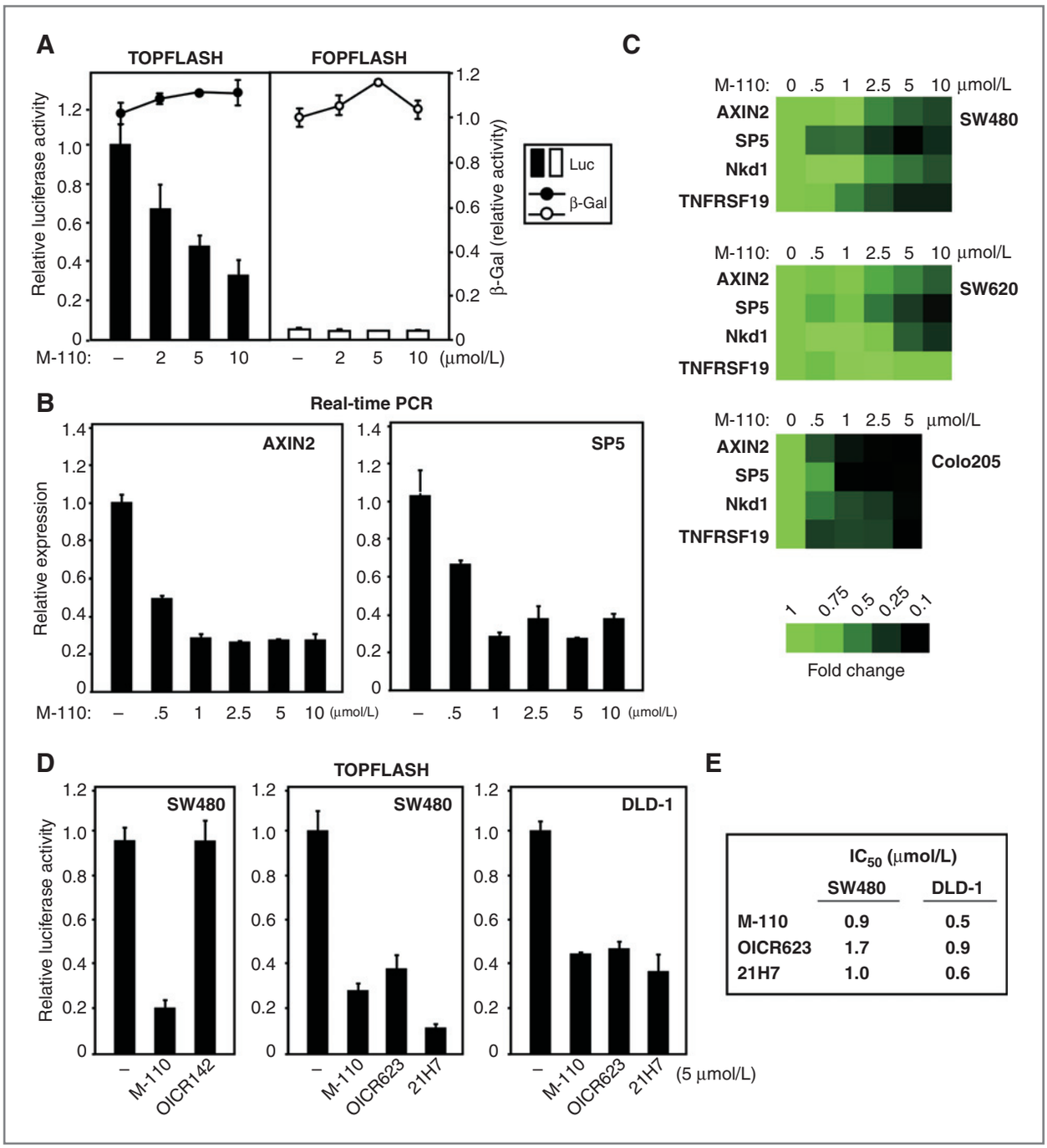

Figure 2. Compounds inhibit constitutive Wnt activity and growth in colon cancer cells. A, inhibition of TOPFLASH by M-110 in DLD-1 cells. Cells were transfected with TOPFLASH or FOPFLASH and treated with the indicated concentration of M-110. Promoter activity was measured by luciferase assay normalized to β-galactosidase activity (bars). β-Galactosidase activities alone are plotted as lines. Data are shown as the mean of 3 replicates ± SD. B and C, M-110 decreases expression of Wnt target genes. Cells were treated with M-110 overnight and the expression of Wnt target genes was measured by real-time PCR. Relative gene expression is plotted as the average of 3 PCR replicates ± the range in DLD-1 cells (B) or as fold change represented by colors (C). D, inhibition of TOPFLASH by M-110, OICR623, 21H7, and the inactive variant, OICR142, was determined in SW480 and DLD-1 cells as in A. E, IC_{50} values for growth inhibition.

A concomitant reduction in Ferritin and increase in TfRI was observed by immunoblotting for M-110 (Fig. 4F) and OICR623, 21H7, and deferasirox (Supplementary Fig. S3A). Thus, given the gene expression profiles and characteristic cell-based responses of iron depletion, our data strongly suggest that OICR623 and related compounds act as iron chelators.

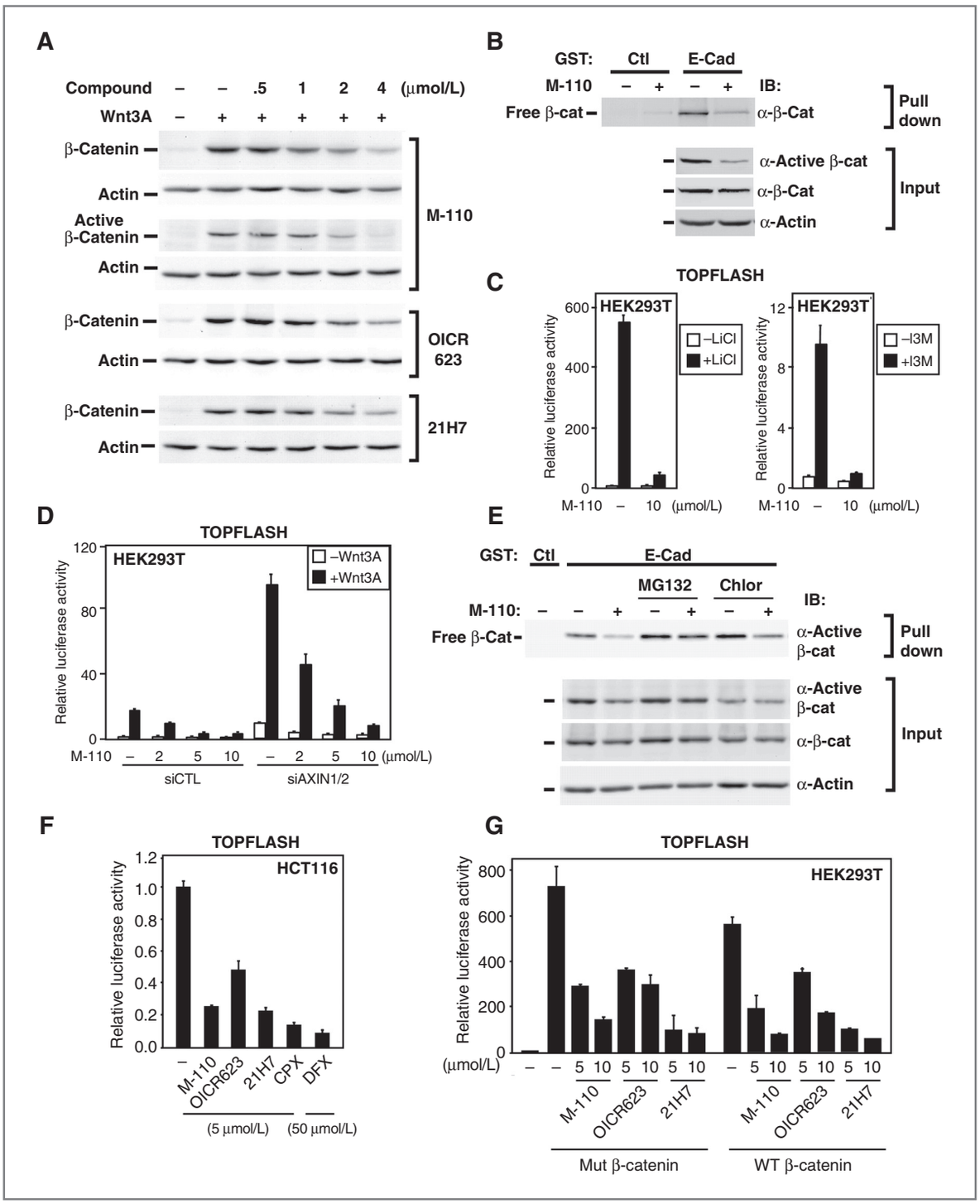

Figure 3. Compounds block Wnt signaling downstream of the destruction complex. A, compounds inhibit Wnt3A-induced stabilization of β-catenin in mouse L cells. Total lysates from cells incubated overnight with DMSO (–) or compounds and then stimulated with Wnt3A for 3 hours were subjected to immunoblotting (IB) to detect total β-catenin, active β-catenin, or β-actin. B, M-110 decreases the level of active β-catenin in colorectal cancer cells. SW480 cells were incubated overnight with 10 μmol/L M-110 and the levels of cytoplasmic (free) β-catenin was determined by GST-E-cadherin (E-Cad) pull down followed by anti-β-catenin IB. Levels of total and active β-catenin in total cell lysates are shown (input). Full-length blots of these cropped images are presented in Supplementary Fig. S4A and B. C and D, inhibition of TOPFLASH downstream of destruction complex components by M-110. HEK293T cells were transfected with TOPFLASH (C and D), siControl (siCtl), or siAXIN1/2 (C) and treated with M-110 with or without 25 mmol/L LiCl or 3M (D). E, the proteasome inhibitor MG132, but not chloroquine, blocks the M-110–mediated decrease in the level of active β-catenin in SW480 cells as determined by E-cadherin pull down assays and immunoblotting as in B. F and G, compounds inhibit TOPFLASH activity in β-catenin mutant, HCT116 cells, and in HEK293T cells overexpressing murine wild-type (WT) or Ser33/Ser37/Thr41/Ser45 to Ala mutant (mut) β-catenin-6xmyc.

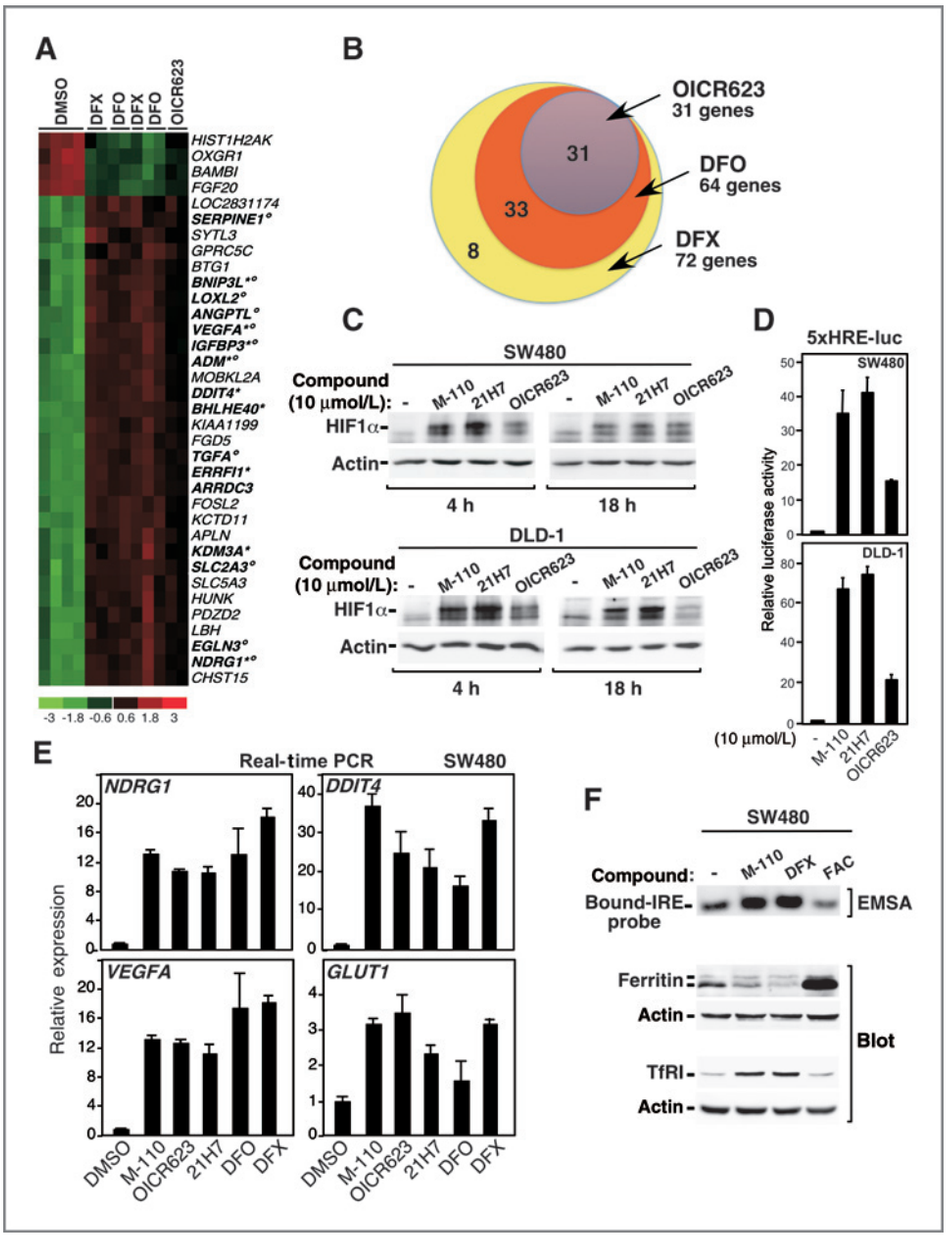

Figure 4. Microarray analysis shows that compounds display an iron chelation gene signature. A, clustering of gene expression profiles of individual runs for all common genes up- or downregulated (>1.5-fold, $P < 0.05$) by OICR623, desferioxamine, and deferasirox are depicted as a heat map matrix. Reported (28, 29) iron-regulated (*) and HIF1α target genes (°) are bolded. B, Venn diagram indicating the number of genes upregulated by OICR623, desferrioxamine (DFO), or deferasirox (DFX) by more than 1.5-fold ($P < 0.05$) is shown. C, SW480 or DLD-1 cells were incubated overnight with 10 μmol/L M-110, and HIF1α protein levels were determined by immunoblotting of total cell lysates. Full-length blots of these cropped images are presented in Supplementary Fig. S4C. D, cells transfected with the 5xHRE-luciferase reporter were treated overnight with M-110 and luciferase activity determined. E, compounds induce expression of iron-responsive target genes. Cells were treated overnight with 5 μmol/L M-110, OICR623, 21H7, 50 μmol/L deferasirox (DFX), or 100 μmol/L desferrioxamine (DFO), and relative expression of target genes, measured by real-time PCR, is plotted as the average of 3 PCR replicates ± the range. F, SW480 cells were incubated with 10 μmol/L M-110, 50 μmol/L deferasirox, or 100 μmol/L FAC, and aliquots of cell lysates were split and analyzed by RNA gel shift assays using a [^{32}P]-human Ferritin H chain IRE probe (electrophoretic mobility shift assay, EMSA) and by immunoblotting to detect Ferritin and TfRI proteins.

Compounds bind iron *in vitro* and in cultured cells and this activity mediates inhibition of Wnt signaling and cell growth

The acyl hydrazone group is a characteristic metal chelating motif, thus, to test whether OICR623 can bind iron *in vitro*, we mixed $Fe(NO_3)_3 \cdot 9H_2O$ with OICR623 and analyzed the mixture by liquid chromatography/mass spectroscopy. An iron complex of OICR623 in a 1:2 ratio (iron:OICR623) with a molecular ion mass [M+1] of 698 was observed. On the basis of the reported crystal and molecular structure of Compound 311 and its iron (III) complex (31), we speculate that OICR623 is a tridendate chelator (Fig. 5A).

We next assessed the ability of the compounds to bind intracellular iron in colorectal cell lines by calcein assay. Upon cell entry, calcein-AM is cleaved into calcein, whose fluorescence is quenched upon chelation of labile iron (23). Calcein-AM–loaded SW480 cells were briefly incubated with M-110, OICR623, and 21H7. Similar to the iron chelator, deferasirox, both M-110 and OICR623 increased calcein fluorescence (Fig. 5B), whereas 21H7 yielded a more modest increase that was similar to that observed for desferioxamine, an iron chelator with poor cell-permeability properties (32). We next tested the effect of excess iron on compound activity in cells. Analysis of TOPFLASH activity in SW480 cells treated with compounds

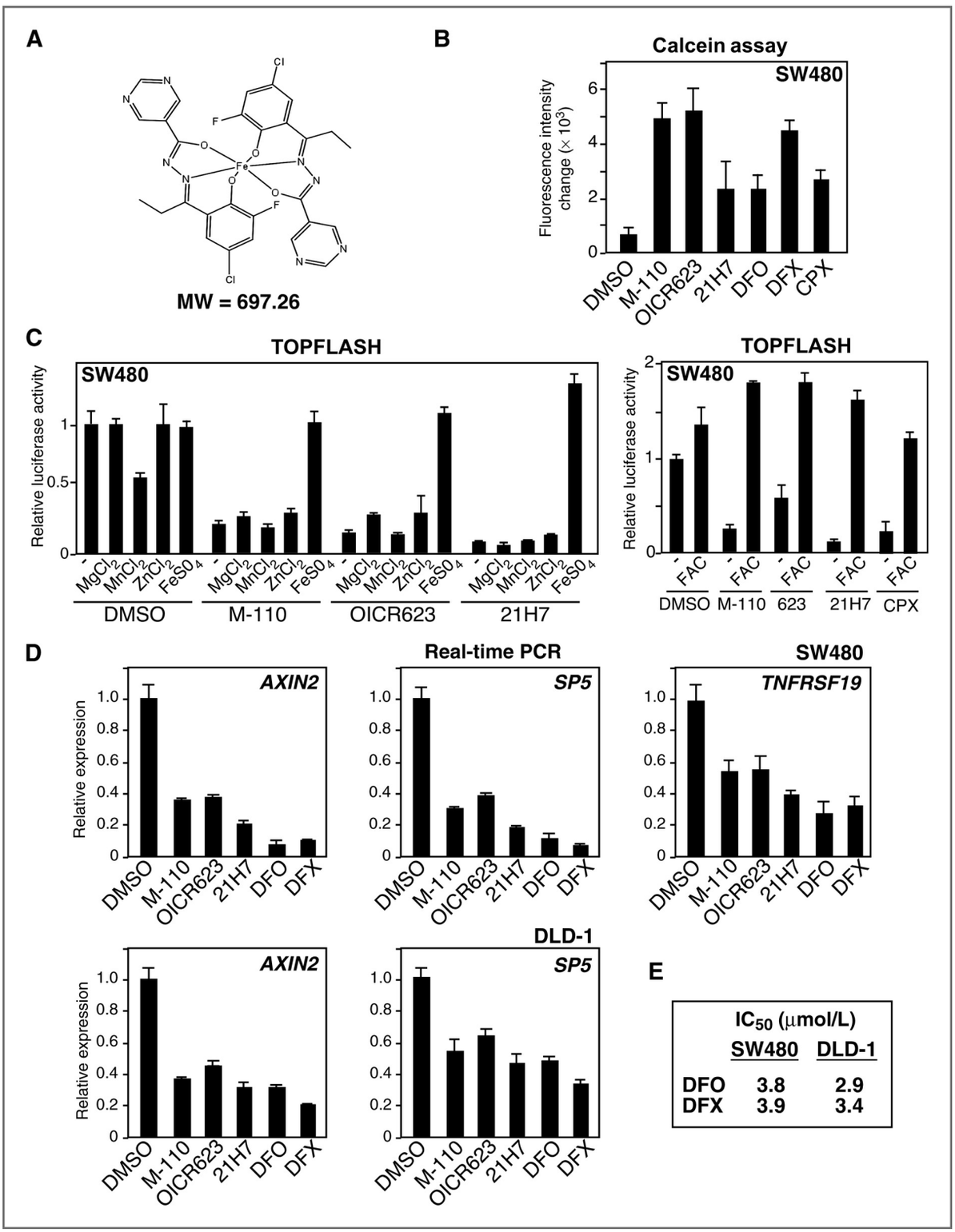

Figure 5. Iron chelators block Wnt signaling and colorectal cancer cell growth. A, a modeled structure of the iron–OICR623 complex. B, compounds bind intracellular iron. SW480 cells were loaded with calcein-AM, and the fluorescence intensity change, after and before the addition of 5 μmol/L M-110, OICR623, 21H7, ciclopirox olamine (CPX), 100 μmol/L desferrioxamine (DFO), or 50 μmol/L deferasirox (DFX) is plotted. C, excess iron blocks compound-mediated inhibition of constitutive Wnt signaling. SW480 cells were transfected with TOPFLASH and treated with 5 μmol/L M-110, OICR623, or 21H7 in the absence or presence of 10 μmol/L of the indicated salts. Promoter activity is shown as the mean of 3 replicates ± SD. D, iron chelators decrease the expression of Wnt target genes. SW480 and DLD-1 cells were treated with 5 μmol/L M-110, OICR623, 21H7, 100 μmol/L desferioxamine, or 100 μmol/L deferasirox overnight, and relative gene expression is plotted as the average of 3 PCR replicates ± the range. E, IC_{50} values for growth inhibition.

(5 μmol/L) coincubated with a 2-fold molar excess (10 μmol/L) of various divalent cations revealed that addition of $FeSO_4$ or FAC completely neutralized compound activity, whereas Mg^{2+}, Mn^{2+}, or Zn^{2+} salts had no effect (Fig. 5C). Moreover, in cell growth assays, addition of $FeSO_4$ at an equimolar ratio of iron to compound completely abrogated the inhibitory activity of the compounds in SW480 and DLD-1 cells (Supplementary Fig. S3B). Treatment of DLD-1 or SW480 cells with the structurally unrelated iron chelators, desferioxamine or deferasirox, similarly inhibited expression of Wnt target genes (Fig. 5D) and inhibited cell growth with IC_{50} values of 2.9 to 3.0 μmol/L (Fig. 5E), roughly 5- to 10-fold higher than the acyl hydrazones, but similar to previously reported IC_{50} values for these compounds (Fig. 5D and E; ref. 33). Stabilization of HIF1α and activation of the HIF1α reporter, 5xHRE-luciferase by DMOG, an inhibitor of 2-oxoglutarate–dependent enzymes including PHDs, to levels (0.1 mmol/L) comparable as that achieved by acyl hydrazones or deferasirox, had no effect on TOPFLASH activity, though at 10-fold higher DMOG doses, some inhibition was observed suggesting that HIF1α is unlikely to be the primary mechanism whereby iron chelators inhibit Wnt signaling (Supplementary Fig. S3C).

Altogether, our results showed that acyl hydrazones are potent iron chelators in cells and that depletion of intracellular iron abrogates cell proliferation and Wnt signaling by promoting β-catenin degradation downstream of the destruction complex.

Oral administration of the iron chelator, ciclopirox olamine, reduces Wnt target gene expression in the leukemic cells of patients with AML

Ciclopirox olamine functions as an anticancer agent in both leukemic cell lines and primary AML patient samples via its intracellular iron chelation activity (34). We confirmed in SW480 cells that ciclopirox olamine also binds intracellular iron (Fig. 5B), induces the HIF1α responsive reporter, and inhibits TOPFLASH in an iron-dependent manner (Fig. 6A and B).

Mutations in Wnt pathway components have not been reported in AML, but expression of β-catenin is correlated with poor prognosis (5). Thus, to determine if iron chelators modulate Wnt signaling *in vivo*, we assessed the effect of systemic administration of ciclopirox olamine to patients with refractory hematologic malignancies. Expression of AXIN2 in patients with AML taking orally administered ciclopirox olamine as part of an on-going phase I dose escalation trial was determined in isolated leukemic blasts. Analysis of samples from 9 patients with relapsed AML receiving ciclopirox olamine doses between 5 and 80 mg/m^2 daily for 5 days revealed that 7 of 9 patients displayed a decrease in AXIN2 levels. For 4 patients (A–D), marked decreases were detected within 1 day of ciclopirox olamine administration (day 2) that became more pronounced from days 3 to 5 (Fig. 6C and D). In 3 patients (E–G), decreases in AXIN2 levels were transient, whereas in 2 patients (H and I), there was no reduction (Fig. 6C and D). Excluding the 2 patients (H and I) who showed no changes, the average reduction in AXIN2 levels from days 2 to 5 ranged from 60% to 74% (median) or 40% to 71% (mean; Fig. 6D). Of note, hematopoietic cells isolated from 2 ciclopirox olamine–administered patients (J–K) with myeloma or MDS, but lacking circulating malignant cells showed no reduction in AXIN2 (Fig. 6E), suggesting that leukemic cells may be more susceptible to iron chelation than non-malignant hematopoietic cells. Although only a small, short-term study, these results show that administration of iron chelators can decrease the expression of Wnt target genes in patients with hematologic malignancies and further indicate that iron chelators might be of therapeutic value for Wnt pathway driven tumors.

Discussion

Stabilization of β-catenin is an invariant feature of cancers with excessive Wnt signaling (1, 2). Our screen, designed to identify small molecules that destabilize β-catenin, identified a compound series that inhibits β-catenin stabilization and blocks Wnt-induced transcription. The compounds were shown to function downstream of the β-catenin destruction complex and were effective in blocking Wnt signaling and growth in APC and β-catenin mutant colorectal cancer cells with constitutive Wnt signaling. This is consistent with studies showing that downregulation of β-catenin inhibits proliferation of colon cancer cell lines grown *in vitro* or as xenografts (35, 36). Given the frequent occurrence of excessive Wnt signaling through a range of mechanisms, these inhibitors which act downstream of the destruction complex to control β-catenin levels could have widespread therapeutic utility in a diverse range of Wnt-driven cancers.

Investigation of the mechanism whereby the acyl hydrazones block the Wnt pathway showed that the compounds bind iron and that this iron chelation activity is essential for compound activity. Iron loading of colorectal cancer cells has been reported to promote Wnt signaling and cell proliferation (37) consistent with our observations that iron depletion can attenuate the pathway. Our conclusions were further supported by the observation that a series of structurally unrelated iron chelators, including desferioxamine, deferasirox, and ciclopirox olamine also inhibit Wnt signaling and that patients with AML taking ciclopirox olamine, show a marked reduction in the expression of the Wnt target gene, AXIN2. Our work along with a recent study (38) show that iron depletion attenuates Wnt signaling, but which of the plethora of iron-dependent proteins, are most relevant for inhibiting Wnt signaling remains to be determined.

Iron is essential for cell growth and metabolism and cancer cells in particular, have an increased demand for iron to maintain cell proliferation having acquired diverse alterations to ensure increased iron accumulation (12–15). In breast cancer, decreases of the intracellular iron exporter, ferroportin, is associated with reduced metastasis-free survival, whereas ferroportin overexpression decreases breast cancer cell growth in an orthotopic mouse model (39). Expression levels of ferroportin are correlated with levels of intracellular iron, indicating that altering iron levels can modulate tumor growth *in vivo*. It is thus tempting to speculate that an increase in iron accumulation promotes widespread increases in the proproliferative Wnt signaling pathway to promote tumorigenesis.

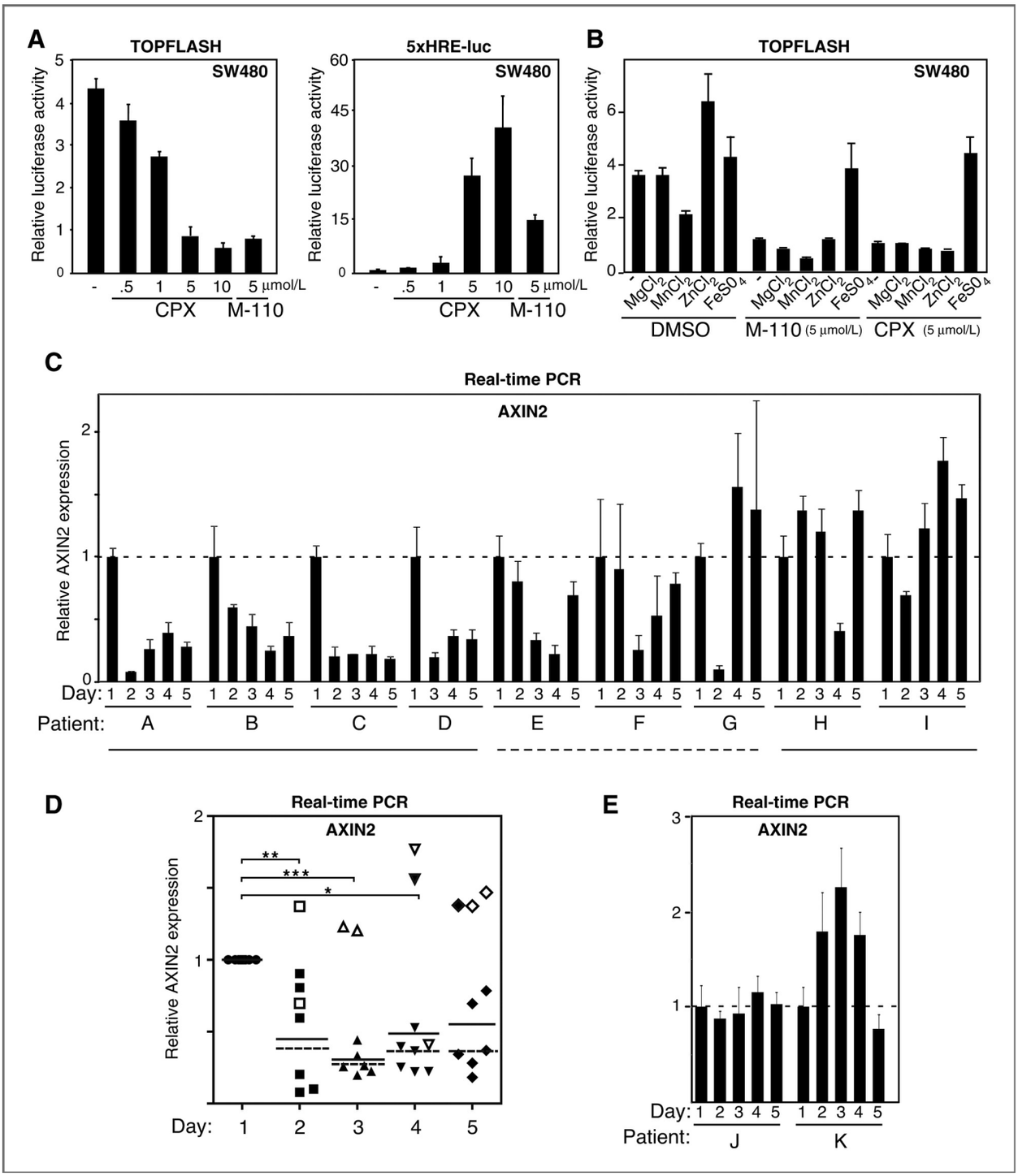

Figure 6. Ciclopirox olamine inhibits Wnt signaling in cultured cells and *in vivo*. A, ciclopirox olamine inhibits Wnt signaling and activates a HIF1α-dependent reporter. SW480 cells transfected with TOPFLASH or 5xHRE-luciferase reporters were treated overnight with ciclopirox olamine or M-110. B, excess iron blocks ciclopirox olamine–mediated inhibition of constitutive Wnt signaling in SW480 cells. Cells were transfected with TOPFLASH and treated with 5 μmol/L ciclopirox olamine in the absence or presence of 10 μmol/L of the indicated salts. C–E, ciclopirox olamine administration decreases AXIN2 expression in leukemic blasts isolated from patients with AML. The expression of AXIN2 on each day of treatment for individual patients was measured by real-time PCR and is calculated relative to levels prior to ciclopirox olamine (CPX) administration. Data for individual patients are plotted as a bar graph (C and E) or scatter plot (D). The horizontal lines indicate the median (dashed line) or mean (solid line) for patients A to G (filled symbols). Results for patients H and I are indicated by open symbols. Probabilities were determined using Student paired, 1-tailed *t* test: ***, $P = 0.008$; **, $P = 0.05$; *, $P = 0.02$. E, AXIN2 expression in 2 patients lacking circulating malignant cells.

Testing the utility of iron chelators, such as the acyl hydrazones identified herein, for cancer therapeutics is an important area for future investigation.

Disclosure of Potential Conflicts of Interest

No potential conflicts of interest were disclosed.

Acknowledgments

The authors thank Rob Donovan, Alessandro Datti, and Thomas Sun at the SMART Robotics Facility; Mark Minden, Andre Schuh, Joseph Brandwein, Vikas Gupta, and Karen Yee of Princess Margaret Hospital for assistance with the clinical trial of ciclopirox olamine; and Jan Jongstra for discussions.

Grant Support

This work was supported by grants from the Ontario Research Fund, the Ontario Cancer Research Network and the Terry Fox Research Institute/Ontario Institute for Cancer Research to L. Attisano and J.L. Wrana and from the Leukemia and Lymphoma Society to A.D. Schimmer. J.L. Wrana and L. Attisano are Canada Research Chairs; J.L. Wrana is an International Scholar of the Howard Hughes Medical Institute; and A.D. Schimmer is a Leukemia and Lymphoma Society Scholar in Clinical Research.

The costs of publication of this article were defrayed in part by the payment of page charges. This article must therefore be hereby marked *advertisement* in accordance with 18 U.S.C. Section 1734 solely to indicate this fact.

Received August 12, 2011; revised October 6, 2011; accepted October 13, 2011; published OnlineFirst October 18, 2011.

References

1. Clevers H. Wnt/beta-catenin signaling in development and disease. Cell 2006;127:469–80.
2. Turashvili G, Bouchal J, Burkadze G, Kolar Z. Wnt signaling pathway in mammary gland development and carcinogenesis. Pathobiology 2006;73:213–23.
3. Nusse R. Wnt signaling and stem cell control. Cell Res 2008;18: 523–7.
4. Majeti R, Becker MW, Tian Q, Lee TL, Yan X, Liu R, et al. Dysregulated gene expression networks in human acute myelogenous leukemia stem cells. Proc Natl Acad Sci U S A 2009;106:3396–401.
5. Ysebaert L, Chicanne G, Demur C, De Toni F, Prade-Houdellier N, Ruidavets JB, et al. Expression of beta-catenin by acute myeloid leukemia cells predicts enhanced clonogenic capacities and poor prognosis. Leukemia 2006;20:1211–6.
6. Wang Y, Krivtsov AV, Sinha AU, North TE, Goessling W, Feng Z, et al. The Wnt/beta-catenin pathway is required for the development of leukemia stem cells in AML. Science 2010;327:1650–3.
7. Barker N, Clevers H. Mining the Wnt pathway for cancer therapeutics. Nat Rev Drug Discov 2006;5:997–1014.
8. Janssens N, Janicot M, Perera T. The Wnt-dependent signaling pathways as target in oncology drug discovery. Invest New Drugs 2006;24:263–80.
9. Chen B, Dodge ME, Tang W, Lu J, Ma Z, Fan CW, et al. Small molecule-mediated disruption of Wnt-dependent signaling in tissue regeneration and cancer. Nat Chem Biol 2009;5:100–7.
10. Huang SM, Mishina YM, Liu S, Cheung A, Stegmeier F, Michaud GA, et al. Tankyrase inhibition stabilizes axin and antagonizes Wnt signalling. Nature 2009;461:614–20.
11. Thorne CA, Hanson AJ, Schneider J, Tahinci E, Orton D, Cselenyi CS, et al. Small-molecule inhibition of Wnt signaling through activation of casein kinase 1alpha. Nat Chem Biol 2010;6:829–36.
12. Kovacevic Z, Kalinowski DS, Lovejoy DB, Yu Y, Rahmanto YS, Sharpe PC, et al. The medicinal chemistry of novel iron chelators for the treatment of cancer. Curr Top Med Chem 2011;11:483–99.
13. Richardson DR, Kalinowski DS, Lau S, Jansson PJ, Lovejoy DB. Cancer cell iron metabolism and the development of potent iron chelators as anti-tumour agents. Biochim Biophys Acta 2009;1790: 702–17.
14. Rouault TA. The role of iron regulatory proteins in mammalian iron homeostasis and disease. Nat Chem Biol 2006;2:406–14.
15. Torti SV, Torti FM. Ironing out cancer. Cancer Res 2011;71:1511–4.
16. Chang M, Kanwar N, Feng E, Siu A, Liu X, Ma D, et al. PIM kinase inhibitors downregulate STAT3(Tyr705) phosphorylation. Mol Cancer Ther 2010;9:2478–87.
17. Labbe E, Lock L, Letamendia A, Gorska AE, Gryfe R, Gallinger S, et al. Transcriptional cooperation between the transforming growth factor-beta and Wnt pathways in mammary and intestinal tumorigenesis. Cancer Res 2007;67:75–84.
18. Miller BW, Lau G, Grouios C, Mollica E, Barrios-Rodiles M, Liu Y, et al. Application of an integrated physical and functional screening approach to identify inhibitors of the Wnt pathway. Mol Syst Biol 2009;5:315.
19. Christova T, Templeton DM. Effect of hypoxia on the binding and subcellular distribution of iron regulatory proteins. Mol Cell Biochem 2007;301:21–32.
20. Skehan P, Storeng R, Scudiero D, Monks A, McMahon J, Vistica D, et al. New colorimetric cytotoxicity assay for anticancer-drug screening. J Natl Cancer Inst 1990;82:1107–12.
21. Winer IS, Bommer GT, Gonik N, Fearon ER. Lysine residues Lys-19 and Lys-49 of beta-catenin regulate its levels and function in T cell factor transcriptional activation and neoplastic transformation. J Biol Chem 2006;281:26181–7.
22. Richardson D, Baker E. Two mechanisms of iron uptake from transferrin by melanoma cells. The effect of desferrioxamine and ferric ammonium citrate. J Biol Chem 1992;267:13972–9.
23. Epsztejn S, Kakhlon O, Glickstein H, Breuer W, Cabantchik I. Fluorescence analysis of the labile iron pool of mammalian cells. Anal Biochem 1997;248:31–40.
24. Ternes N, Scheiber-Mojdehkar B, Landgraf G, Goldenberg H, Sturm B. Iron availability and complex stability of iron hydroxyethyl starch and iron dextran a comparative *in vitro* study with liver cells and macrophages. Nephrol Dial Transplant 2007;22:2824–30.
25. Smyth GK. Linear models and empirical bayes methods for assessing differential expression in microarray experiments. Stat Appl Genet Mol Biol 2004;3:Article3.
26. Yang J, Zhang W, Evans PM, Chen X, He X, Liu C. Adenomatous polyposis coli (APC) differentially regulates beta-catenin phosphorylation and ubiquitination in colon cancer cells. J Biol Chem 2006; 281:17751–7.
27. Brembeck FH, Rosario M, Birchmeier W. Balancing cell adhesion and Wnt signaling, the key role of beta-catenin. Curr Opin Genet Dev 2006;16:51–9.
28. Saletta F, Rahmanto YS, Noulsri E, Richardson DR. Iron chelator-mediated alterations in gene expression: identification of novel iron-regulated molecules that are molecular targets of hypoxia-inducible factor-1 alpha and p53. Mol Pharmacol 2010;77:443–58.
29. Semenza GL. Hypoxia-inducible factor 1: oxygen homeostasis and disease pathophysiology. Trends Mol Med 2001;7:345–50.
30. Keith B, Simon MC. Hypoxia-inducible factors, stem cells, and cancer. Cell 2007;129:465–72.
31. Richardson DR, Bernhardt PV. Crystal and molecular structure of 2-hydroxy-1-naphthaldehyde isonicotinoyl hydrazone (NIH) and its iron (III) complex: an iron chelator with anti-tumour activity. J Biol Inorg Chem 1999;4:266–73.
32. Ihnat PM, Vennerstrom JL, Robinson DH. Synthesis and solution properties of deferoxamine amides. J Pharm Sci 2000;89:1525–36.
33. Green DA, Antholine WE, Wong SJ, Richardson DR, Chitambar CR. Inhibition of malignant cell growth by 311, a novel iron chelator of the pyridoxal isonicotinoyl hydrazone class: effect on the R2 subunit of ribonucleotide reductase. Clin Cancer Res 2001;7:3574–9.

34. Eberhard Y, McDermott SP, Wang X, Gronda M, Venugopal A, Wood TE, et al. Chelation of intracellular iron with the antifungal agent ciclopirox olamine induces cell death in leukemia and myeloma cells. Blood 2009;114:3064–73.
35. Roh H, Green DW, Boswell CB, Pippin JA, Drebin JA. Suppression of beta-catenin inhibits the neoplastic growth of APC-mutant colon cancer cells. Cancer Res 2001;61:6563–8.
36. van de Wetering M, Sancho E, Verweij C, de Lau W, Oving I, Hurlstone A, et al. The beta-catenin/TCF-4 complex imposes a crypt progenitor phenotype on colorectal cancer cells. Cell 2002;111:241–50.
37. Brookes MJ, Boult J, Roberts K, Cooper BT, Hotchin NA, Matthews G, et al. A role for iron in Wnt signalling. Oncogene 2008;27:966–75.
38. Coombs GS, Schmitt AA, Canning CA, Alok A, Low IC, Banerjee N, et al. Modulation of Wnt/beta-catenin signaling and proliferation by a ferrous iron chelator with therapeutic efficacy in genetically engineered mouse models of cancer. Oncogene 2011 Jun 13 [Epub ahead of print].
39. Pinnix ZK, Miller LD, Wang W, D'Agostino R Jr, Kute T, Willingham MC, et al. Ferroportin and iron regulation in breast cancer progression and prognosis. Sci Transl Med 2010;2:43ra56.